

Assessment of a Coulomb-attenuated exchange-correlation energy functional

Michael J G Peach^a, Trygve Helgaker^b, Paweł Sałek^c,
Thomas W Keal^a, Ola B Lutnæs^b, David J Tozer^a, Nicholas C Handy^d

^aDepartment of Chemistry, University of Durham,
South Road, Durham, DH1 3LE UK.

^bDepartment of Chemistry, University of Oslo,
PO Box 1033, Blindern, N-0315 Oslo, Norway

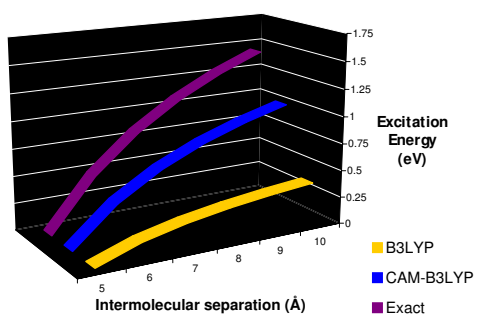
^cLaboratory of Theoretical Chemistry, AlbaNova University Center,
Royal Institute of Technology, S-10691 Stockholm, Sweden

^dDepartment of Chemistry, University of Cambridge,
Lensfield Road, Cambridge, CB2 1EW UK.

Email: D.J.Tozer@Durham.ac.uk

Fax: 0191 384 4737

October 7, 2005



The performance of the Coulomb-attenuated CAM-B3LYP exchange-correlation functional is compared with that of B3LYP in an extensive chemical assessment.

Abstract

The recently-proposed CAM-B3LYP exchange-correlation energy functional, based on a partitioning of the r_{12}^{-1} operator in the exchange interaction into long- and short-range components, is assessed for the determination of molecular thermochemistry, structures, and second-order response properties. Rydberg and charge-transfer excitation energies and static electronic polarisabilities are notably improved over the standard B3LYP functional; classical reaction barriers also improve. Ionisation potentials, bond lengths, NMR shielding constants and indirect spin-spin coupling constants are comparable with the two functionals. CAM-B3LYP atomisation energies and diatomic harmonic vibrational wavenumbers are less accurate than those of B3LYP. Future research directions are outlined.

1 Introduction and theoretical background

Yanai *et al.* [1] recently introduced a new hybrid exchange-correlation energy functional for Kohn-Sham density functional theory (DFT), based on the Coulomb-attenuating method (CAM). The approximation, denoted CAM-B3LYP, follows original works of Hirao and coworkers [2, 3] and Savin and coworkers [4, 5]; see Refs. [6-9] for related work. Preliminary investigations [1, 10] have demonstrated that CAM-B3LYP provides significantly improved Rydberg and charge-transfer electronic excitation energies, due to an improved description of the long-range exchange interaction. However, there has been minimal investigation into its performance for other chemical properties. The present study addresses this issue.

We commence by reiterating the definition of the functional, taking the opportunity to clarify in greater detail some of its aspects. It is recognised that a crucial part of an exchange-correlation functional is the exchange component. The key step in the Coulomb-attenuating method of Ref. [1] is the partitioning of the r_{12}^{-1} operator, in the exchange interaction, into two parts

$$\frac{1}{r_{12}} = \frac{[\alpha + \beta \operatorname{erf}(\mu r_{12})]}{r_{12}} + \frac{1 - [\alpha + \beta \operatorname{erf}(\mu r_{12})]}{r_{12}} \quad (1)$$

where μ is a parameter of dimension L^{-1} and α and β are dimensionless parameters satisfying $0 \leq \alpha + \beta \leq 1$, $0 \leq \alpha \leq 1$, and $0 \leq \beta \leq 1$. The exchange energy is then expressed as the sum of long-range (LR) and short-range (SR) components

$$E_{\text{x}} = E_{\text{x}}^{\text{LR}} + E_{\text{x}}^{\text{SR}} \quad (2)$$

The long-range part is evaluated quantum mechanically, in terms of spin orbitals

$$E_{\text{x}}^{\text{LR}} = \alpha E_{\text{x}}^0 - \frac{\beta}{2} \sum_{\sigma} \sum_{ij} \int \int \psi_{i\sigma}(\mathbf{r}_1) \psi_{j\sigma}(\mathbf{r}_1) \frac{\operatorname{erf}(\mu r_{12})}{r_{12}} \psi_{i\sigma}(\mathbf{r}_2) \psi_{j\sigma}(\mathbf{r}_2) d\mathbf{r}_1 d\mathbf{r}_2 \quad (3)$$

where E_x^0 is the exact, negative, orbital exchange energy (the standard Hartree-Fock expression evaluated using the Kohn-Sham orbitals) whilst the short-range part is expressed in terms of the local DFT one-particle density matrix $P_{1\sigma}(\mathbf{r}_1, \mathbf{r}_2)$

$$E_x^{\text{SR}} = -\frac{1}{2} \sum_{\sigma} \int \int \frac{(1 - [\alpha + \beta \text{erf}(\mu r_{12})]) (P_{1\sigma}(\mathbf{r}_1, \mathbf{r}_2))^2}{r_{12}} d\mathbf{r}_1 d\mathbf{r}_2 \quad (4)$$

The notation LR and SR reflects the dependence of the partitioning in Eqn. (1) on the interelectron distance r_{12} , as is evident in Fig. 2(c) of Ref. [1]. As r_{12} gets larger, the exchange is increasingly described through the exact orbital expression, rather than through density functional theory. From Eqn. (3), an exact description of long-range exchange ($r_{12} \rightarrow \infty$) requires $\alpha + \beta = 1$.

For the case of the local density approximation (LDA) in the short-range component, changing variables to $\mathbf{r} = (\mathbf{r}_1 + \mathbf{r}_2)/2$ and $\mathbf{s} = \mathbf{r}_1 - \mathbf{r}_2$ and performing the \mathbf{s} integration (which can be performed analytically as shown by Gill *et al* [11]), gives the following result

$$E_x^{\text{SR}} = -\frac{1}{2} \sum_{\sigma} \int \rho_{\sigma}^{4/3} K_{\sigma}^{\text{LDA}} \left((1 - \alpha) - \beta \left(\frac{8}{3} a_{\sigma} \left[\sqrt{\pi} \text{erf} \left(\frac{1}{2a_{\sigma}} \right) + 2a_{\sigma} (b_{\sigma} - c_{\sigma}) \right] \right) \right) d\mathbf{r} \quad (5)$$

where K_{σ}^{LDA} is defined by the standard LDA exchange energy expression

$$E_x^{\text{LDA}} = -\frac{1}{2} \sum_{\sigma} \int \rho_{\sigma}^{4/3} K_{\sigma}^{\text{LDA}} d\mathbf{r} \quad (6)$$

and a_{σ} , b_{σ} , c_{σ} are given by

$$a_{\sigma} = \frac{\mu}{2k_{\sigma}^{\text{LDA}}} \quad (7)$$

$$b_{\sigma} = \exp\left(-\frac{1}{4a_{\sigma}^2}\right) - 1 \quad (8)$$

$$c_{\sigma} = 2a_{\sigma}^2 b_{\sigma} + \frac{1}{2} \quad (9)$$

k_{σ}^{LDA} is the Fermi momentum

$$k_{\sigma}^{\text{LDA}} = (6\pi^2 \rho_{\sigma})^{1/3} \quad (10)$$

which is related to K_{σ}^{LDA} by

$$k_{\sigma}^{\text{LDA}} = (9\pi/K_{\sigma}^{\text{LDA}})^{1/2} \rho_{\sigma}^{1/3} \quad (11)$$

To derive an approximate short-range energy expression for generalised gradient approximation (GGA) functionals, Ikura *et al.* [2] assumed that the GGA one-particle density matrix could be obtained by evaluating the LDA matrix with the modified momentum

$$k_{\sigma}^{\text{GGA}} = (9\pi/K_{\sigma}^{\text{GGA}})^{1/2} \rho_{\sigma}^{1/3} \quad (12)$$

where K_σ^{GGA} defines the GGA energy in an analogous manner to Eqn. (6). This gives

$$E_x^{\text{SR}} = -\frac{1}{2} \sum_\sigma \int \rho_\sigma^{4/3} K_\sigma^{\text{GGA}} \left((1 - \alpha) - \beta \left(\frac{8}{3} a_\sigma \left[\sqrt{\pi} \operatorname{erf} \left(\frac{1}{2a_\sigma} \right) + 2a_\sigma (b_\sigma - c_\sigma) \right] \right) \right) d\mathbf{r} \quad (13)$$

where $a_\sigma = \mu/2k_\sigma^{\text{GGA}}$. CAM-B3LYP uses the Becke 1988 (B88) exchange functional [12]

$$K_\sigma^{\text{GGA}} = K_\sigma^{\text{LDA}} + \frac{2\beta_B x_\sigma^2}{1 + 6\beta_B x_\sigma \operatorname{arcsinh} x_\sigma} \quad (14)$$

with $\beta_B = 0.0042$ and $x_\sigma^2 = (\nabla\rho_\sigma)^2/\rho_\sigma^{8/3}$. Eqn. (13) can alternatively be written

$$E_x^{\text{SR}} = (1 - \alpha) E_x^{\text{GGA}} + \frac{4\beta}{3} \sum_\sigma \int \rho_\sigma^{4/3} K_\sigma^{\text{GGA}} a_\sigma \left[\sqrt{\pi} \operatorname{erf} \left(\frac{1}{2a_\sigma} \right) + 2a_\sigma (b_\sigma - c_\sigma) \right] d\mathbf{r} \quad (15)$$

When $\beta = 0$, the total (short-range plus long-range) exchange energy reduces to $E_x = \alpha E_x^0 + (1 - \alpha) E_x^{\text{GGA}}$, demonstrating that this new exchange functional has a close connection to the exchange part of the classic B3LYP [13-15] functional (although it is not identical even when $\alpha = 0.2$, see section 3). Therefore, a natural choice for the correlation component of CAM-B3LYP is the B3LYP correlation term

$$E_c = \gamma E_c^{\text{LYP}} + (1 - \gamma) E_c^{\text{VWN5}} \quad (16)$$

with $\gamma = 0.81$ [15, 16]. This correlation functional, combined with the short- and long-range exchange components, with fitted values of $\alpha = 0.19$, $\beta = 0.46$, and a value of $\mu = 0.33 a_0^{-1}$ following Ikura *et al.* [2] (but see discussion later), completely defines the CAM-B3LYP functional. In Section 2, a detailed assessment of CAM-B3LYP is presented, comparing with the results from the standard B3LYP. Conclusions and future research directions are presented in Section 3.

2 Assessment of the CAM-B3LYP functional

The preliminary assessments [1, 10] of the CAM-B3LYP functional considered electronic excitation energies, together with a relatively small number of atomisation energies, ionisation potentials, and total energies. We now expand the assessment to a much wider range of properties and molecules. Specifically we consider atomisation energies, ionisation potentials, classical reaction barriers, bond lengths of covalent molecules and hydrogen-bonded dimers, harmonic vibrational wavenumbers, NMR shielding constants and indirect spin-spin coupling constants, static electronic polarisabilities, and electronic excitation energies from time-dependent DFT. Table 1 lists the molecules considered in each assessment.

Table 2 lists mean and mean absolute errors, relative to reference values (experimental or correlated *ab initio*) for B3LYP and CAM-B3LYP.

Assessments 1, 2, 4, 5, 6, 7, and 10 consider subsets of the molecules considered in Ref. [17]. Assessment 3 (classical reaction barriers) considers a subset of the BH42/04 database of Zhao *et al.* [18]. Assessments 8 and 9 (NMR shielding constants and spin-spin couplings) consider the molecules in Ref. [19]. Assessment 11 (localised excitation energies) considers N₂ and CO as in Ref. [20]. Assessment 12 considers the dipeptide excitations of Ref. [21]. For Assessment 3, calculations were performed at the QCISD geometries of Ref. [18] using the 6-311+G(3df,2p) basis set. For all other assessments, the same basis sets, geometries, and reference values were used as in the original studies. As a final assessment, we also consider the C₂H₄ ··· C₂F₄ charge transfer (CT) excitation investigated by Dreuw *et al.* [22], using BLYP [12, 15] geometries and the TZ2P basis set [23]. All calculations were performed using a pre-release version of the DALTON program [24], using a restricted formalism for open-shell systems.

The α and β parameters defining CAM-B3LYP were determined through a fit to the atomisation energies of (essentially) the G2-1 set of molecules [25]. Yanai *et al.* [1] demonstrated that for these molecules, CAM-B3LYP atomisation energies are of comparable quality to those of B3LYP. Assessment 1 of the present study considers a subset of the full G2 set of molecules [25, 26], involving many larger systems. The CAM-B3LYP error is now more than twice as large as that of B3LYP, indicating that the high quality is not maintained outside the fitting data. Assessment 2 considers ionisation potentials; in line with the observations of Yanai *et al.* [1], CAM-B3LYP is slightly less accurate than B3LYP. Assessment 3 considers classical reaction barriers, which are known to be a significant challenge for approximate DFT functionals [27, 28]. The CAM-B3LYP mean absolute error of 2.1 kcal mol⁻¹ is notably smaller than that of B3LYP (2.8 kcal mol⁻¹). The ‘average’ amount of exact orbital exchange (averaged over all interelectron distances) is larger in CAM-B3LYP than B3LYP; it is well-established that increasing the fraction of exact orbital exchange improves the reaction barriers of systems such as those in this assessment, for example see Ref. [29].

Assessments 4, 5, and 6 consider bond lengths of covalent molecules and hydrogen-bonded dimers. CAM-B3LYP bond lengths tend to be shorter than those of B3LYP. This leads to improved quality for the diatomic set, but a degradation for the hydrogen bonded dimers and G2 molecules, where the shortening is excessive. The shortening is also evident in the overestimated CAM-B3LYP harmonic vibrational wavenumbers of Assessment 7. Assessments 8 and 9 consider nuclear magnetic resonance (NMR) shielding constants and indirect spin-spin coupling constants, determined in the conventional manner. CAM-B3LYP and B3LYP provide comparable quality.

Assessments 10-12 consider second-order electric response properties. For the static isotropic polarisabilities in Assessment 10, CAM-B3LYP is a notable improvement over B3LYP, which is consistent with the long-range nature of this property. Assessment 11 considers localised (non CT) excitations. CAM-B3LYP is a significant improvement over B3LYP, which can be traced to improved Rydberg excitations. Assessment 12 considers excitation energies of a model dipeptide. CAM-B3LYP is again a notable improvement, which can this time be traced to the description of the intramolecular CT excitation. It is well-established that long-range exact orbital exchange is important for CT excitations [22, 30]. Following Dreuw *et al.* [22], we have also considered the asymptotic dependence of the lowest intermolecular CT excitation energy between two isolated molecules (C_2H_4 and C_2F_4) on the distance between the molecules R . Figure 1 compares calculated curves with the exact $-\frac{1}{R}$ behaviour, which arises from the electrostatic interaction between the charged species following excitation. The behaviour of the curves is completely dominated by the description of the exchange at large interelectron distances. B3LYP therefore exhibits a $-\frac{0.2}{R}$ dependence, whilst CAM-B3LYP exhibits an improved $-\frac{\alpha+\beta}{R} = -\frac{0.65}{R}$.

Figure 1 demonstrates that the values of α and β defining CAM-B3LYP are not optimal for asymptotic intermolecular CT excitations. They are also not optimal for Rydberg excitations. Using parameters modified so that $\alpha+\beta = 1$ (specifically, $\alpha = 0.19$, $\beta = 0.81$) will clearly improve the behaviour in Figure 1. We have confirmed that it also improves the Rydberg excitations of Assessment 11; the mean absolute error reduces to 0.24 eV. However, such a functional cannot be recommended for general use since the individual parameters α and β are not optimised. Atomisation energies and barriers are very poor (errors in excess of 10 kcal mol⁻¹) and bond lengths are severely shortened. Interestingly, the dipeptide excitations also degrade ($|d| = 0.69$ eV); the intramolecular CT excitation in this molecule is shorter ranged than the excitation in Figure 1.

3 Conclusions and future research directions

We have examined the performance of the CAM-B3LYP exchange-correlation energy functional for the evaluation of a wide range of molecular properties. The key observation is the improvement in long-range properties such as Rydberg and CT excitation energies, and electronic polarisabilities. This improvement is not associated with any significant increase in computational cost. For several other properties, CAM-B3LYP is comparable to B3LYP. For some properties, most notably atomisation energies, CAM-B3LYP cannot compete with B3LYP.

Further investigation of Coulomb-attenuated functionals is now required. CAM-

B3LYP is far from optimal and we are confident that further improvements can be made. We highlight three areas that must be addressed. First, we have demonstrated the importance of the $\alpha + \beta = 1$ condition; future Coulomb-attenuated functionals must incorporate such a condition in order to further improve long-range excitations. Second, the choice of GGA exchange and correlation functionals is not optimal; the scheme must be applied to newer forms such as Becke's 1997 expansion [31]. The choice of expansion highlights an important observation regarding the gradient corrected exchange in the present study. The exchange contribution in the B3LYP functional can be written

$$E^{\text{B3LYP}} = A \cdot E_{\text{x}}^0 + (1 - A) \cdot E_{\text{x}}^{\text{LDA}} + B \cdot \Delta E_{\text{x}}^{\text{B88}} \quad (17)$$

where $A = 0.2$, $B = 0.72$ and $\Delta E_{\text{x}}^{\text{B88}}$ is the B88 gradient correction. For $\beta = 0$ (no attenuation), the CAM-B3LYP exchange functional takes the form

$$E^{\text{CAM-B3LYP}} = \alpha \cdot E_{\text{x}}^0 + (1 - \alpha) \cdot E_{\text{x}}^{\text{LDA}} + (1 - \alpha) \cdot \Delta E_{\text{x}}^{\text{B88}} \quad (18)$$

with $\alpha = 0.19$. Thus, even if α is reset to 0.2, the two functionals will not be identical due to the different pre-factors of the B88 gradient correction; to reduce to B3LYP, the underlying exchange term in CAM-B3LYP would have to be $E_{\text{x}}^{\text{GGA}} = E_{\text{x}}^{\text{LDA}} + 0.9\Delta E_{\text{x}}^{\text{B88}}$, rather than $E_{\text{x}}^{\text{GGA}} = E_{\text{x}}^{\text{LDA}} + \Delta E_{\text{x}}^{\text{B88}}$. (We note that the CAM-B3LYP case is analogous to that of B1LYP [32]). This discussion leads us to consider an alternative approach, where the Coulomb-attenuation is applied to the local density exchange only, such that the short-range term is given by Eqn. (5). A gradient corrected exchange term and a correlation functional could then be added, and their parameters optimised. Such a procedure would remove the assumption of Ikura *et al.* [2], that the GGA one particle density matrix can be obtained from a momentum scaling and would bring the functional closer to the more usual GGA and hybrid forms, in the sense that they augment the (attenuated) LDA functional. The disadvantage of such an approach is that the GGA exchange would not be eliminated completely as $r_{12} \rightarrow \infty$, as the (small) gradient correction would remain.

A third area that must be addressed is the choice of μ in Eqn. (1) and its relationship to the expansion parameters defining the functional. Preliminary studies on electronic excitations in the hydrogen atom show that the CAM-B3LYP time-dependent excitation spectrum is an improvement over B3LYP when its original parameters are used ($\alpha + \beta = 0.65$, $\mu = 0.33 \text{ a}_0^{-1}$). If we constrain $\alpha + \beta = 1.0$, then μ must be reduced, in order not to degrade the shape of the attenuation in the smaller r_{12} region. For hydrogen, a value of $\mu = 0.15 \text{ a}_0^{-1}$ is more appropriate. We are investigating these three issues.

4 Acknowledgments

We are grateful to T. Yanai for providing benchmark CAM-B3LYP energies for testing the DALTON implementation and to the EPSRC for studentship support (TWK). The work has received support from the Norwegian Research Council through a Strategic University Program in Quantum Chemistry (Grant No. 154011/420) and through a grant of computer time from the program for Supercomputing.

Table 1: Systems used in the 12 assessments; see Table 2 for the corresponding errors.

1. Atomisation energies

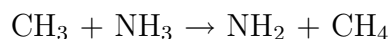
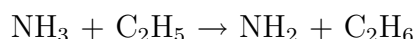
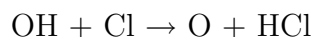
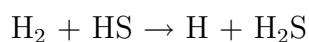
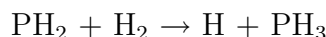
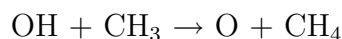
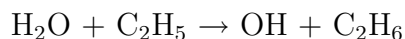
Acetamide, acetic acid, acetone, acetyl chloride, acetyl fluoride, acrylonitrile, AlCl_3 , allene, aziridine, BCl_3 , BeH , benzene, BF_3 , bicyclobutane, C_2H_2 , C_2H_3 , C_2H_4 , C_2H_5 , C_2H_6 , CCH , CF_3CN , CF_4 , CH , $\text{CH}_2(^1A)$, CH_2CHF , CH_3 , $(\text{CH}_3)_2\text{CH}$, $(\text{CH}_3)_3\text{C}$, $\text{CH}_3\text{CH}_2\text{O}$, CH_3Cl , CH_3CO , CH_3O , CH_3OH , CH_4 , CHF_3 , Cl_2 , ClF , ClNO , CO , CO_2 , cyclobutene, cyclopropene, dimethylamine, dimethylether, ethanol, ethylchloride, F_2 , F_2O , formic acid, furan, H_2 , H_2CO , H_2COH , H_2O , H_2O_2 , HCl , HCO , HF , HOCl , isobutane, isopropanol, ketene, Li_2 , LiF , LiH , methyl cyanide, methyl ethylether, methyl formate, methyl nitrite, methylamine, methylene cyclopropane, N_2 , N_2O , Na_2 , NaCl , NF_3 , NH_3 , nitromethane, NO_2 , O_3 , OH , oxirane, propane, propylchloride, propyne, pyridine, pyrrole, trans-ethylamine, trimethylamine, 2-butyne, vinylchloride.

2. Ionisation potentials

Li , Be , B , C , N , O , F , Na , Mg , Al , CH_4 , NH_3 , H_2O , HF , HCl , C_2H_2 , C_2H_4 , CO , N_2 , Cl_2 , ClF .

3. Classical reaction barriers

$\text{CH}_3 + \text{H}_2 \rightarrow \text{CH}_4 + \text{H}$
 $\text{OH} + \text{CH}_4 \rightarrow \text{CH}_3 + \text{H}_2\text{O}$
 $\text{H} + \text{H}_2 \rightarrow \text{H}_2 + \text{H}$
 $\text{OH} + \text{NH}_3 \rightarrow \text{H}_2\text{O} + \text{NH}_2$
 $\text{HCl} + \text{CH}_3 \rightarrow \text{Cl} + \text{CH}_4$
 $\text{OH} + \text{C}_2\text{H}_6 \rightarrow \text{H}_2\text{O} + \text{C}_2\text{H}_5$
 $\text{F} + \text{H}_2 \rightarrow \text{HF} + \text{H}$
 $\text{O} + \text{HCl} \rightarrow \text{OH} + \text{Cl}$
 $\text{NH}_2 + \text{CH}_3 \rightarrow \text{CH}_4 + \text{NH}$
 $\text{NH}_2 + \text{C}_2\text{H}_5 \rightarrow \text{C}_2\text{H}_6 + \text{NH}$
 $\text{C}_2\text{H}_6 + \text{NH}_2 \rightarrow \text{NH}_3 + \text{C}_2\text{H}_5$
 $\text{NH}_2 + \text{CH}_4 \rightarrow \text{CH}_3 + \text{NH}_3$
 $s\text{-trans cis-}\text{C}_5\text{H}_8 \rightarrow s\text{-trans cis-}\text{C}_5\text{H}_8$
 $\text{H}_2 + \text{Cl} \rightarrow \text{H} + \text{HCl}$
 $\text{CH}_4 + \text{H} \rightarrow \text{CH}_3 + \text{H}_2$
 $\text{H}_2\text{O} + \text{NH}_2 \rightarrow \text{OH} + \text{NH}_3$
 $\text{Cl} + \text{CH}_4 \rightarrow \text{HCl} + \text{CH}_3$



4. Diatomic bond lengths

Li_2 , LiNa , LiK , Na_2 , NaK , K_2 , N_2 , NP , NAS , P_2 , PAS , As_2 , F_2 , FCl , FBr , Cl_2 , ClBr , Br_2 , LiF , LiCl , NaF , NaCl , NaBr , KF , KCl , BCl , BBr , AlF , AlCl , AlBr , CO , CS , CSe , SiO , SiS , SiSe , GeO , GeS .

5. Hydrogen bond dimer distances

$(\text{HF})_2$, $(\text{HCl})_2$, $(\text{H}_2\text{O})_2$, $(\text{CO})(\text{HF})$, $(\text{OC})(\text{HF})$.

6. G2 Bond lengths

H_2 , LiH , $\text{CH}_2(^1A)$, NH_3 , H_2O , HF , Li_2 , LiF , C_2H_2 , C_2H_4 , HCN , CO , H_2CO , N_2 , H_2O_2 , F_2 , CO_2 , HCl , Na_2 , Cl_2 , NaCl , SiO , CS , ClF .

7. Harmonic vibrational wavenumbers

Li_2 , LiNa , LiK , Na_2 , NaK , K_2 , N_2 , NP , NAS , P_2 , PAS , As_2 , F_2 , FCl , Cl_2 , ClBr , Br_2 , LiF , LiCl , NaF , NaCl , NaBr , KF , KCl , BCl , BBr , AlF , AlCl , AlBr , CO , CS , CSe , SiO , SiS , SiSe , GeO , GeS .

8. Isotropic NMR shielding constants

CF_2 , CF_4 , NO_2^- , linear CO_2 , cyclic CO_2 , linear N_2O , cyclic N_2O , cis- N_2F_2 , trans- N_2F_2 , C_6H_6 , C_2H_3^+ , C_7H_9^+ , $\text{C}_6\text{H}_5\text{N}_2^+$, HF , N_2 , H_2O , CO , HCN , CH_4 , C_2H_2 , C_2H_4 .

9. Indirect spin-spin coupling constants

HF , CO , N_2 , H_2O , HCN , NH_3 , CH_4 , C_2H_2 , C_2H_4 , C_2H_6 , C_6H_6 .

10. Isotropic polarisabilities

HF , F_2 , CO , N_2 , CH_4 , CO_2 , C_2H_4 , PH_3 , H_2O , H_2S , SO_2 , HCl , Cl_2 .

11. Localised excitation energies

CO , N_2 .

12. Dipeptide excitation energies

$\text{C}_5\text{N}_2\text{O}_2\text{H}_{10}$.

Table 2: Mean error d and mean absolute error $|d|$ for the systems in Table 1. (Error = calculated – reference).

| | B3LYP | CAM-B3LYP |
|---|-------|-----------|
| 1. Atomisation energies | | |
| $d/\text{kcal mol}^{-1}$ | 0.5 | 4.8 |
| $ d /\text{kcal mol}^{-1}$ | 2.2 | 5.5 |
| 2. Ionisation potentials | | |
| d/eV | 0.03 | 0.13 |
| $ d /\text{eV}$ | 0.15 | 0.18 |
| 3. Classical reaction barriers | | |
| $d/\text{kcal mol}^{-1}$ | -2.4 | -0.9 |
| $ d /\text{kcal mol}^{-1}$ | 2.8 | 2.1 |
| 4. Diatomic bond lengths | | |
| $d/\text{\AA}$ | 0.013 | -0.007 |
| $ d /\text{\AA}$ | 0.017 | 0.014 |
| 5. Hydrogen bond dimer distances | | |
| $d/\text{\AA}$ | 0.01 | -0.03 |
| $ d /\text{\AA}$ | 0.04 | 0.06 |
| 6. G2 bond lengths | | |
| $d/\text{\AA}$ | 0.003 | -0.007 |
| $ d /\text{\AA}$ | 0.008 | 0.011 |
| 7. Harmonic vibrational wavenumbers | | |
| d/cm^{-1} | 6 | 34 |
| $ d /\text{cm}^{-1}$ | 22 | 37 |
| 8. Isotropic NMR shielding constants | | |
| d/ppm | -37.1 | -36.5 |
| $ d /\text{ppm}$ | 37.1 | 36.5 |
| 9. Indirect spin-spin coupling constants | | |
| d/Hz | 1.4 | 1.3 |
| $ d /\text{Hz}$ | 8.0 | 7.3 |
| 10. Isotropic polarisabilities | | |
| d/au | 0.36 | 0.15 |
| $ d /\text{au}$ | 0.45 | 0.30 |
| 11. Localised excitation energies | | |
| d/eV | -0.82 | -0.45 |
| $ d /\text{eV}$ | 0.82 | 0.46 |
| 12. Dipeptide excitation energies | | |
| d/eV | -0.15 | 0.39 |
| $ d /\text{eV}$ | 0.73 | 0.40 |

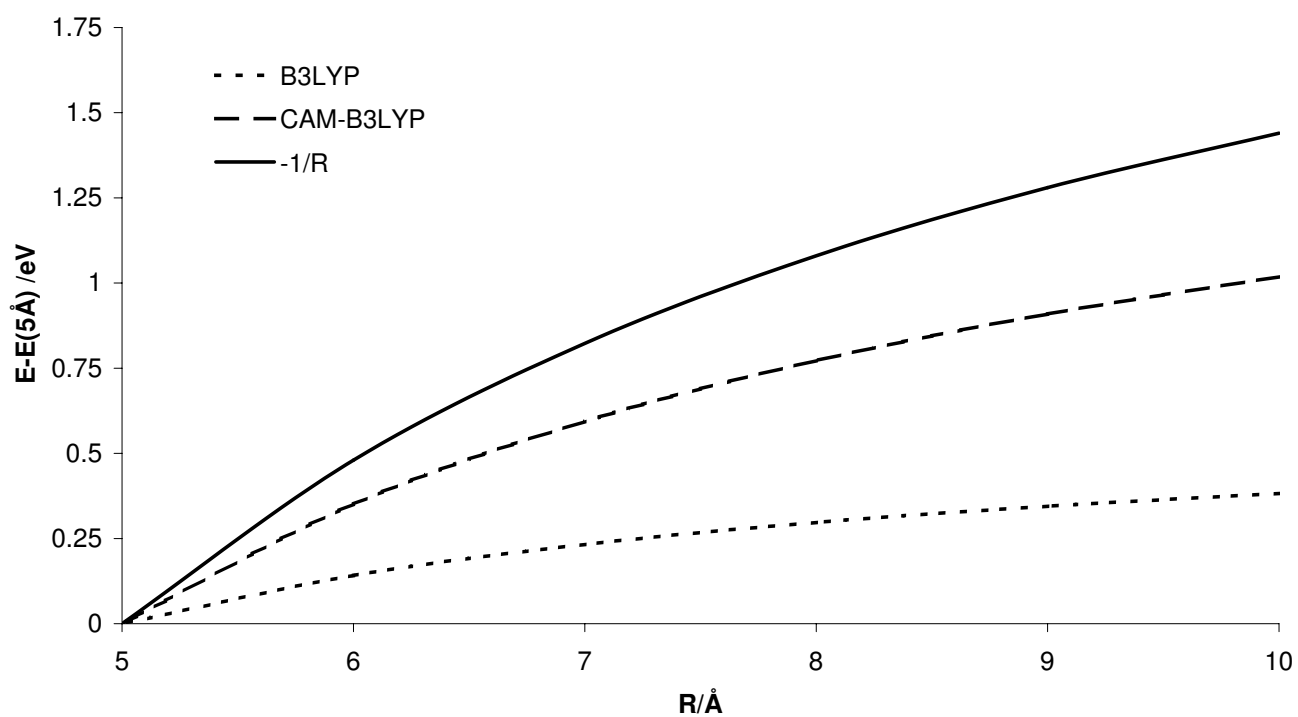


Figure 1: Charge transfer excitation energy of $\text{C}_2\text{H}_4 \cdots \text{C}_2\text{F}_4$ as a function of intermolecular distance, R , with B3LYP and CAM-B3LYP functionals. The excitation energy at 5 \AA is set to zero for all methods.

References

- [1] T. Yanai, D. P. Tew, and N. C. Handy. *Chem. Phys. Lett.* **393** 51 (2004)
- [2] H. Ikura, T. Tsuneda, T. Yanai, and K. Hirao. *J. Chem. Phys.* **115** 3540 (2001)
- [3] Y. Tawada, T. Tsuneda, S. Yanagisawa, T. Yanai, and K. Hirao. *J. Chem. Phys.* **120** 8425 (2004)
- [4] A. Savin, in: J. M. Seminario, Ed, *Recent Developments and Applications of Modern Density Functional Theory*, Elsevier, Amsterdam (1996)
- [5] T. Leininger, H. Stoll, H.-J. Werner, and A. Savin. *Chem. Phys. Lett.* **275** 151 (1997)
- [6] M. Kamiya, T. Tsuneda, and K. Hirao. *J. Chem. Phys.* **117** 6010 (2002)
- [7] J. Heyd, G. E. Scuseria, and M. Ernzerhof. *J. Chem. Phys.* **118** 8207 (2003)
- [8] J. Toulouse, F. Colonna, and A. Savin. *Phys. Rev. A.* **70** 062505 (2004)
- [9] R. Baer and D. Neuhauser. *Phys. Rev. Lett.* **94** 043002 (2005)
- [10] T. Yanai, R. J. Harrison, and N. C. Handy. *Molec. Phys.* **103** 413 (2005)
- [11] P. M. W. Gill, R. D. Adamson, and J. A. Pople. *Molec. Phys.* **88** 1005 (1996)
- [12] A. D. Becke. *Phys. Rev. A.* **38** 3098 (1988)
- [13] A. D. Becke. *J. Chem. Phys.* **98** 5648 (1993)
- [14] P. J. Stephens, F. J. Devlin, C. F. Chabalowski, and M. J. Frisch. *J. Phys. Chem.* **98** 11623 (1994)
- [15] C. Lee, W. Yang, and R. G. Parr. *Phys. Rev. B.* **37** 785 (1988)
- [16] S. J. Vosko, L. Wilk, and M. Nusair. *Can. J. Phys.* **58** 1200 (1980)
- [17] T. W. Keal and D. J. Tozer. *J. Chem. Phys.* **121** 5654 (2004)
- [18] Y. Zhao, B. J. Lynch, and D. G. Truhlar. *J. Phys. Chem. A* **108** 2715 (2004)
- [19] T. W. Keal, D. J. Tozer, and T. Helgaker. *Chem. Phys. Lett.* **391** 374 (2004)
- [20] D. J. Tozer and N. C. Handy. *J. Chem. Phys.* **109** 10180 (1998)
- [21] D. J. Tozer, R. D. Amos, N. C. Handy, B. O. Roos, and L. Serrano-Andrés. *Molec. Phys.* **97** 859 (1999)

- [22] A. Dreuw, J. L. Weisman, and M. Head-Gordon. *J. Chem. Phys.* **119** 2943 (2003)
- [23] T. H. Dunning, Jr.. *J. Chem. Phys.* **55** 716 (1971); S. Huzinaga, *ibid.* **42** 1293 (1965)
- [24] DALTON, a molecular electronic structure program, Release 2.0 (2005), see <http://www.kjemi.uio.no/software/dalton/dalton.html>.
- [25] L. A. Curtiss, K. Raghavachari, G. W. Trucks, and J. A. Pople. *J. Chem. Phys.* **94** 7221 (1991)
- [26] L. A. Curtiss, K. Raghavachari, P. C. Redfern, and J. A. Pople. *J. Chem. Phys.* **106** 1063 (1997)
- [27] S. Skokov and R. A. Wheeler. *Chem. Phys. Lett.* **271** 251 (1997)
- [28] M. Filatov and W. Thiel. *Chem. Phys. Lett.* **295** 467 (1998)
- [29] B. J. Lynch, P. L. Fast, M. Harris, and D. G. Truhlar. *J. Phys. Chem. A.* **104** 4811 (2000)
- [30] D. J. Tozer. *J. Chem. Phys.* **119** 12697 (2003)
- [31] A. D. Becke. *J. Chem. Phys.* **107** 8554 (1997)
- [32] C. Adamo and V. Barone. *Chem. Phys. Lett.* **274** 242 (1997)